Hyperfine Interact (2007) 174:97–102
DOI 10.1007/s10751-007-9570-z

Status of the TRIμP project

Results of commissioning experiments

H. W. Wilschut · U. Dammalapati · S. De · P. Dendooven · O. Dermois · K. Jungmann · A. J. Mol · C. J. G. Onderwater · A. Rogachevskiy · M. da Silva · M. Sohani · E. Traykov · L. Willmann

Published online: 11 July 2007

Abstract At KVI the technical structures for the TRIμP facility are nearly all in place. The aim of the project is to use radioactive ions to study fundamental interactions and symmetries. We will measure β-recoil correlations in nuclear β decay. There the V,A structure of the Weak interaction may be violated. The second line of research is the search for a permanent electric dipole moment in Ra, with a magnitude forbidden by the Standard Model. By trapping these radioactive nuclei in atom traps a pure sample that can be manipulated facilitates these searches. The TRIμP facility consists of a production target and magnetic separator on the high energy side and a Radio-Frequency Quadrupole (RFQ) cooler and buncher on the low energy side. An ion catcher stops the fast product nuclides and transport them into the RFQ cooler. New technological approaches were implemented for several of these devices.

Keywords Radioactive ion and atom trapping · Magnetic separator · Production mechanisms · Magneto-Optical traps

1 Introduction

Rare and short-lived radio isotopes are of interest because of their nuclear properties. They offer unique possibilities for investigating fundamental physical symmetries, for applied physics, and for nuclear structure studies [1]. The main motivation

H. W. Wilschut (✉) · U. Dammalapati · S. De · P. Dendooven · O. Dermois · K. Jungmann · A. J. Mol · C. J. G. Onderwater · A. Rogachevskiy · M. da Silva · M. Sohani · E. Traykov · L. Willmann
Kernfysisch Verneller Instituut, University of Groningen, Groningen, The Netherlands
e-mail: wilschut@kvi.nl

for investigating fundamental symmetries is to improve limits for the validity of the Standard Model, as it can be inferred from high-precision measurements. Such low energy experiments are complementary to searches for new physics in High-Energy physics experiments. In particular, high accuracy can be achieved, when suitable radioactive isotopes can be cooled and stored in atom or ion traps [2–5].

With this aim the TRIμP (Trapped Radioactive Isotopes: μicrolaboratories for fundamental Physics) facility at the Kernfysisch Versneller Instituut(KVI) in Groningen, The Netherlands, was proposed and funded in order to provide a state of the art user facility for such high-precision studies. In particular it is intended to use atomic traps for such studies. Here we report on some recent aspects associated with constructing and commissioning of various parts of the facility.

2 The magnetic separator and inverse reaction kinematics

The first part of the TRIμP facility, the dual magnetic separator, has been completed and commissioned. Details are described in [6]. Secondary beams produced to date are ^{22}Mg, ^{21}Na, ^{20}Na, ^{19}Ne, ^{12}N, and ^{12}B using (p,n) charge exchange and deuteron stripping reactions in inverse kinematics. Typical yields are $10^3 - 10^4$ particles/s per particle nA of beam using a H_2 or D_2 gas target at a pressure of 1 bar. The maximum beam current has been 60 particle nA so far. Two very different production strategies have been used, which we shortly discuss below. More details are given in [7].

In non-relativistic kinematics the contributing momentum range ($\Delta p/p$) in a binary reaction is

$$\frac{\Delta p}{p} = 2\sqrt{\frac{A_{TLF}A_T}{A_{PLF}A_P}\left(1+\frac{Q}{E_{cm}}\right)}. \tag{1}$$

Here A_T and A_{TLF} are the light target and outgoing target-like fragment and mass, respectively, while A_P and A_{PLF} are the heavy projectile and the product projectile-like masses. In reactions where the Q-value is much smaller than the center-of-mass energy ($|Q| \ll E_{cm}$), the momentum range only depends on the masses of the particles and not on the energy. For example in a (p,n) reaction $\Delta p/p = 2/A_P$. Because reactions of interest have often large negative Q-values, the kinetic energy of the fragment can still be high enough for separator operation. In addition the cross sections approaching the reaction threshold have often large resonant-like yields. The typical momentum dependence observed in that case is shown in Fig. 1 for the reaction ^{20}Ne(p,n)^{20}Na at 22.3 MeV/nucleon, which has a Q=-14.7 MeV. The typical forward/backward structure of the distribution is mainly due the angular opening of the separator. The data are for two angular openings, the curves indicate a Monte Carlo calculation that incorporates multiple scattering and straggling contributions.

A completely different production strategy is based on direct reactions. Here one exploits that the cross sections mainly depend on the momentum transfer, which is particularly true in charge exchange reactions. Consequently, the angular distributions are increasingly focused with increasing energy. The higher energy also allows to use thicker targets and compensates the decrease of the cross section with energy. All considerations are discussed in [7]. In Fig. 2 typical momentum distributions are shown for a stripping and a charge exchange reaction, showing the narrow

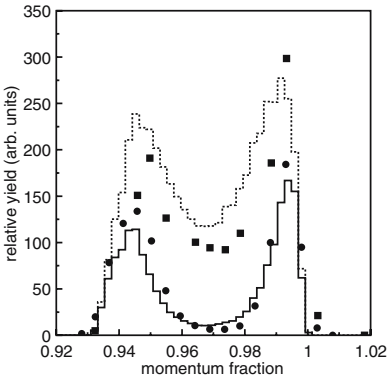

Fig. 1 Momentum dependence of the measured ^{20}Na yield for two angular openings of the separator. The *filled circles* correspond to an angular opening of 32 mrad and the filled squares to the maximum angular opening of 60 mrad. The histograms show the result of Monte Carlo simulations assuming isotropic emission. The *full* and dashed histogram refer to the *small* and *large opening*, respectively. The relative normalization of the two data sets is uncertain due to systematic errors of about 20%

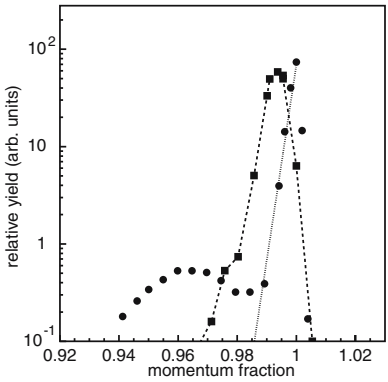

Fig. 2 Momentum dependence of the reactions p(^{21}Ne,^{21}Na)n at 43 MeV/nucleon and d(^{20}Ne,^{21}Na)n at 22.3 MeV/nucleon. The result for the first reaction is indicated by the *filled circles*. The *dotted line* through the *sharp rising part* of the distribution is a fit to obtain information on the first diffraction peak of the angular distribution. The *filled squares* give the distribution of the stripping reaction; the *dashed line* connecting these data points is to guide eye

momentum bite of these reactions. The separator is thus completely operational. The secondary beams are either used to develop the low energy apparatus of the TRIμP facility, or have also been used for experiments.

3 Ion catcher

The ion catcher is a compact thermal ionizer. Originally a He-gas filled ion catcher was foreseen. However, this would appear to have led to severe rate limitations [8].

Even when rate limitations do not play a role the fraction of surviving ions in the stopping process remains well below 100%. In a cryogenic test (maximal reduction of contaminants) the survival fraction of ionized Rn in different noble gasses remained below 30% [9]. From the stopping of Hydrogen in Helium it is known that Hydrogen is continuously neutralized and ionized in the stopping process [10]. What factors determine the freeze-out of this process and at which energy it occurs is as yet not known.

As the radioactive products eventually will need to be trapped in atom traps, it is mostly alkali and earth alkali atoms that are of interest. For these reasons, with the loss of generality, a thermal ionizer was chosen as high-energy ion stopper. For these elements very high extraction efficiencies have consistently been reported [11]. The stopper/thermal ionizer we are developing consists of tungsten foils inside a tungsten cavity that can be heated, An electric field gradient allows extraction through the exit aperture. Details are described in [12]. We have used ^{20}Na for testing. This isotope is convenient because it has a short life time ($T_{1/2} = 0.448$ s) and decays with a branching of 16% by α particles. Switching the primary beam on and off and measuring the time dependence of the α particles production, an effective half life of the source was deduced to be about 1 s. So far we have reached efficiencies of about 5% for ^{20}Na, for ^{21}Na ($T_{1/2} = 22.5$ s) this should be at least a factor 5 higher. Improving the design to increase the efficiency are in progress.

4 Radio frequency cooler and buncher

The ion catcher is followed by a Radio Frequency Quadrupole (RFQ) cooler and buncher. This buncher has a novel design which minimizes the wiring and vacuum feedtroughs. The RFQ cooler and buncher have been tested with a ^{23}Na ion beam. The buncher will be used to accumulate particles which allows them to be transported without the need for a high voltage platform. The cooler and also the buncher efficiency was measured to be nearly 60%. The longitudinal cooling time (required for bunching) was about 1 ms, delivering bunches of at least $5 \cdot 10^4$ particles. More details are in [12].

5 Atom trapping

5.1 Collector MOT

One project that our group is working on is the measurement of $\beta - \nu$ correlations in β decay with the final aim to measure the time reversal violating D coefficient. The neutrino information is inferred from the recoiling nucleus. The sample being studied will reside in a Magneto-Optical Trap (MOT), as has been done for ^{21}Na [13] and ^{38}K^m [14], to be able to measure the recoiling ion. We are currently developing the trapping system. We have chosen for dual setup with a collector and detection MOT cf. [14]. The collector MOT consist of small glass volume which allows optimal ratio laser beam volume versus chamber volume. The walls are coated with dry-film. A neutralizer of Y is used to catch the incoming ions and emit them as atoms . We test the setup with a low-energy beam of stable ^{23}Na ions. A typical observation is

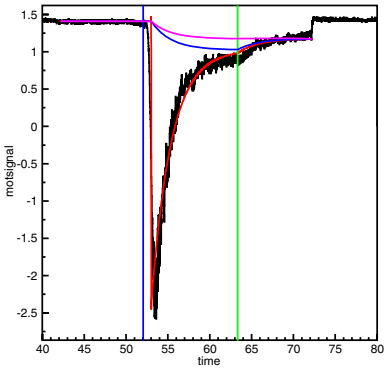

Fig. 3 (Color on-line) The measured MOT signal (*inverted*) as function of time. *Left* of the first *vertical line* (*blue*) the neutralizer heater is off; on the *right* it is on. The ion beam is on for about 65 s then it is switched off (second line (*green*)). The first contribution (*magenta*) is due to Na released slowly by the heater. The second is associated with the ion-beam current (*blue*, last term (2)). The third and main contribution is that of the accumulated beam being heated from the neutralizer surface (*red*, first term of (2))

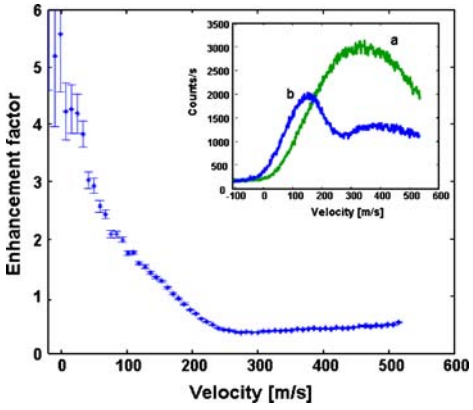

Fig. 4 (Color on-line) Enhancement of flux of slow atoms due to laser cooling

shown in Fig. 3, where the MOT signal as function of time is shown. The signal can be modeled as

$$N_{\mathrm{MOT}} = \alpha_c \tau_p I(\Delta t \exp(-t/\tau_t) + \tau_t(1 - \exp(-t/\tau_t)), \tag{2}$$

where α_c is the capture rate, I is the beam current, τ_p the characteristic time the Na atoms are available as a gas and τ_t the rate at which atoms are removed from the MOT cloud due to background collisions. The main effect is the release of atoms when the neutralizer heater is turned on after accumulation over a time Δt, given by the first term in (2). The second term describes the contribution of the beam current converted directly into a MOT signal, reaching the equilibrium value $\alpha_c \tau_p I \tau_t$. The relative contribution of the two components is $\Delta t/\tau_t$. In these derivations $\tau_p \ll \tau_t$. As a final contribution we note that the heater will continuously release Na which is here assumed to reach a constant rate. The three contributions listed above are shown accumulatively in Fig. 3. The function thus required a three parameter fit. Currently

we did not exceed the single pass efficiency for the trapping rate. The complications due the residual Na background will be resolved once radioactive ions are available.

5.2 Barium cooling

To prepare for radium trapping, first the technical approach is studied with the chemical homologue barium. The only option for laser cooling is offered by the $^1S_0$ - $^1P_1$ transition. The main difference compared to other successfully laser cooled atoms arises from the decay into metastable D states. On an average an atom scatters 340 photons on the $^1S_0$ - $^1P_1$ transition before it will decay into one of the metastable states and the atom is removed from the cooling cycle. This corresponds to a velocity change of only 1.5 m/s, not enough for efficient laser cooling. This obstacle can be overcome by using additional lasers to drive the atoms from the metastable states back into the ground state. This repumping is done by lasers at 1,500 and 1,130 nm.

The velocity distribution of the atomic beam from a Ba oven is measured by observing the Doppler shift of the $^1S_0$ - $^1P_1$ transition induced by a weak probe 553.7 nm laser beam at 45° with respect to atomic beam. Curve *a* in the inset of Fig. 4 shows the Maxwell–Boltzmann velocity distribution of the Ba atomic beam measured with the probe laser. Curve *b* was obtained with the repump lasers and the strong cooling laser directed against the atomic beam. The shift in velocity of the atoms is about 60 m/s. This corresponds (see Fig. 4) to an enhancement of slow atoms by a factor 5. This shows that with the use of repumpers, laser cooling of atoms with complex level schemes is feasible. Details are in [15] The next step is to trap barium atoms in a MOT.

6 Conclusion

We are currently in the last stages to produce a radioactive beam that can be trapped as atoms in a MOT. We expect to start the scientific research programme in the beginning of 2007.

References

1. NuPECC Report: NuPECC Long Range Plan 2004: Perspectives for Nuclear Physics Research in Europe in the Coming Decade and Beyond. Available from http://www.nupecc.org/pub/
2. Turkstra, J.W., Wilschut, H.W., Meyer, D., Hoekstra, R., Morgenstern, R.: Hyperfine Interact. **127**, 533 (2000)
3. Jungmann, K.: Acta Phys. Pol. **33**, 2049 (2002)
4. Wilschut, H.W.: Hyperfine Interact. **146/147**, 77 (2003)
5. Jungmann, K.: Nucl. Phys. A **751**, 87c (2005)
6. Berg, G.P.A., et al.: Nucl. Instrum. Methods A **560**, 169 (2006)
7. Traykov, E., et al.: Nucl. Instrum. Meth. A **572**, 580 (2007)
8. Huyse, M., et al.: Nucl. Instrum. Methods B **187**, 535 (2002)
9. Dendooven, P., Purushothaman, S., Gloos, K.: Nucl. Instrum. Meth. A **558**, 580 (2006)
10. Olivera, G.H., et al.: Phys. Rev. A **49**, 603 (1994); Instrum. Methods A **558**, 580 (2005)
11. Kirchner, R.: Nucl. Instrum. Methods A **292**, 203 (1990)
12. Traykov, E.: Thesis, University of Groningen (2006)
13. Scielzo, N.D., et al.: Phys. Rev. Lett. **93**, 102501 (2004)
14. Gorelov, A., et al.: Phys. Rev. Lett. **94**, 142501 (2005)
15. Dammalapati, U.: Thesis, Universtity of Groningen (2006)